Supporting Information

# Laser Direct Writing of Carbonaceous Sensors on Cardboard toward Human Health Monitoring and Indoor Environment Monitoring

*Kuan Ju[a], Yang Gao[a,]*, Ting Xiao[a], Cunjiang Yu[b], Jianpin Tan[a], Fuzhen Xuan[a,]**

[a]School of Mechanical and Power Engineering, East China University of Science and Technology, Shanghai 200237 (China)

[b]Department of Mechanical Engineering, University of Houston, Houston, TX 77204 (USA)

*E-mail: yanggao@ecust.edu.cn (Yang Gao); fzxuan@ecust.edu.cn (Fuzhen Xuan)

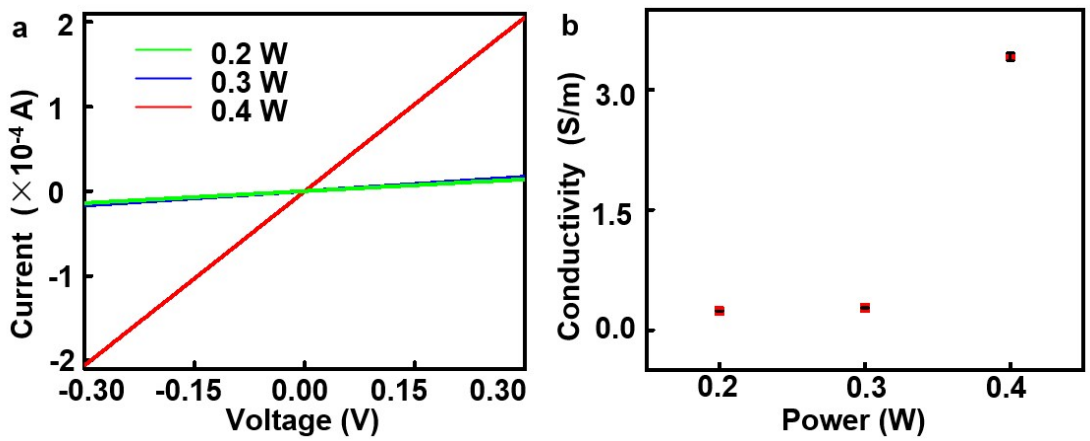


**Figure S1.** Conductivity of the dumbbell pattern resistance strip fabricated by LDW. (a) I-V curves of the dumbbell pattern resistance strip fabricated by LDW at Pw of 0.2, 0.3 and 0.4 W. (b) The conductivity of the carbonaceous pattern on cardboard fabricated by LDW at laser power of 0.2, 0.3 and 0.4 W.

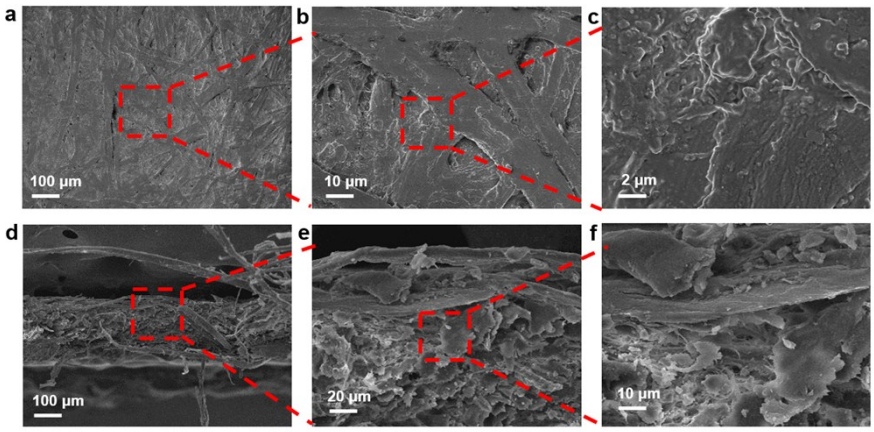


**Figure S2.** SEM images of the pristine cardboard. (a-c) SEM images of the pristine cardboard surface. (d-f) Cross-sectional SEM images of the pristine cardboard.

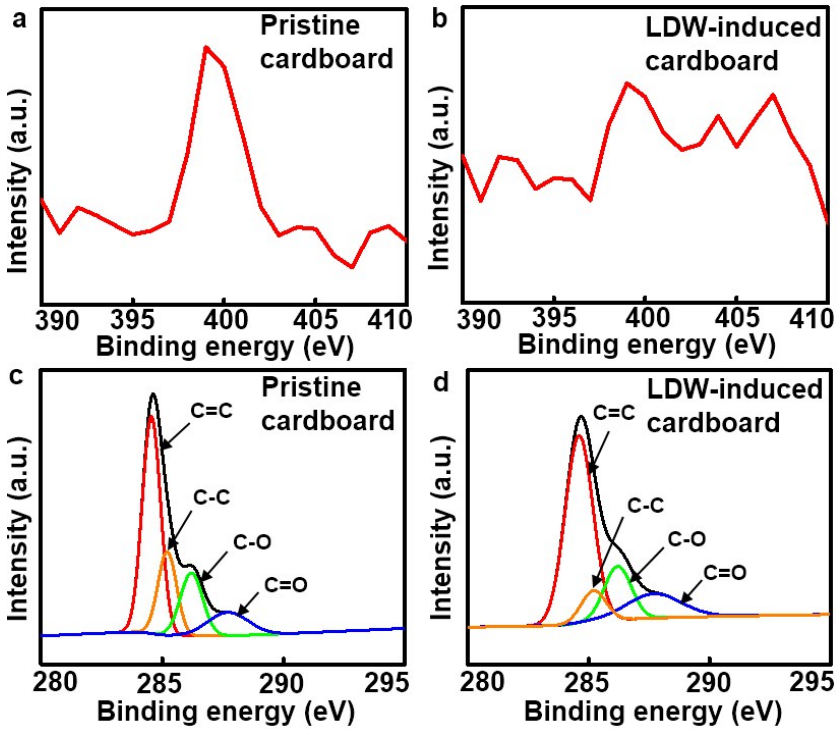


**Figure S3.** Carbonization mechanism of the LDW-induced cardboard. (a) N1s XPS spectra of the pristine cardboard. (b) N1s XPS spectra of the LDW-induced cardboard. (c) High-resolution C1s XPS spectra of the pristine cardboard. (d) High-resolution C1s XPS spectra of the LDW-induced cardboard. C=C – 284.6 eV, C-C – 285.2 eV, C-O – 286.2 eV, C=O – 287.7 eV.

.

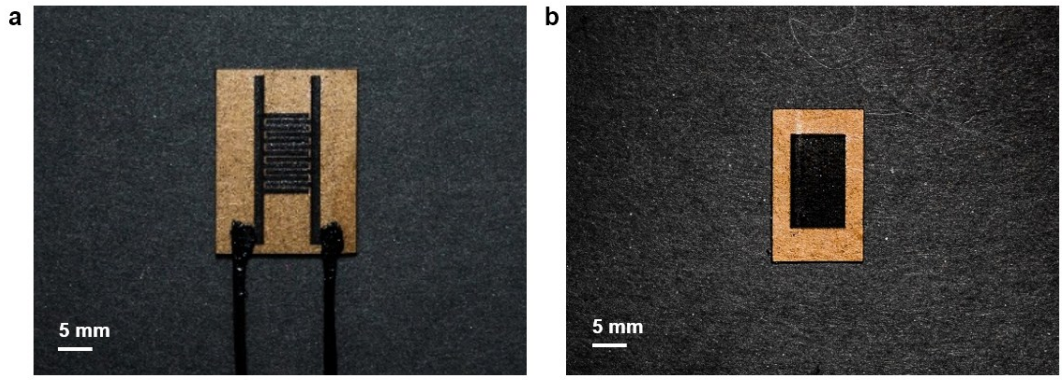


**Figure S4.** Photographs exhibiting a LDW-carbonized pressure sensor. (a) A photograph exhibiting a LDW-Carbonized interdigital electrode formed on a piece of cardboard. (b) A photograph exhibiting a LDW-carbonized conductive layer with a rectangular shape.

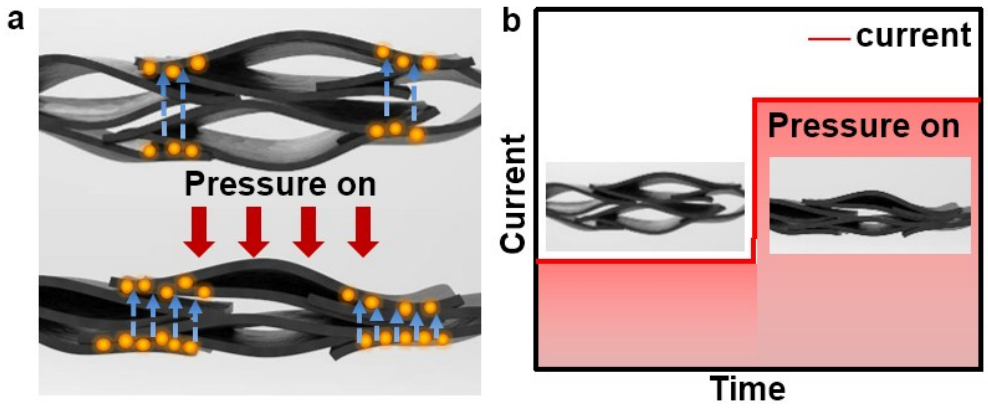


**Figure S5.** Schematic diagram of the sensing mechanism of the device. (a) A schematic diagram exhibiting the pressure-response mechanism of the carbonized cardboard sensor in which and the layered carbonaceous flakes is used as the conductive region. (b) A schematic demonstrating the conductive of the device improves under pressure.

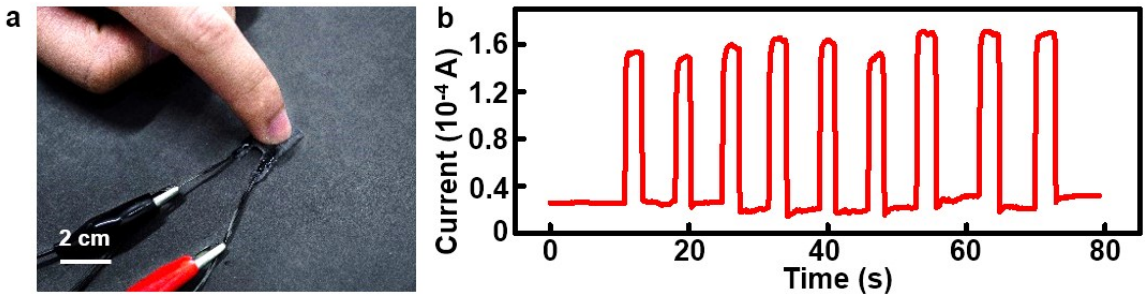


**Figure S6.** The tactile pressure sensing performance of sensors. (a) Photograph demonstrating the LDW-carbonized sensor detecting pressing force. (b) Current response plot of the device resulting from pressing loading cycles.

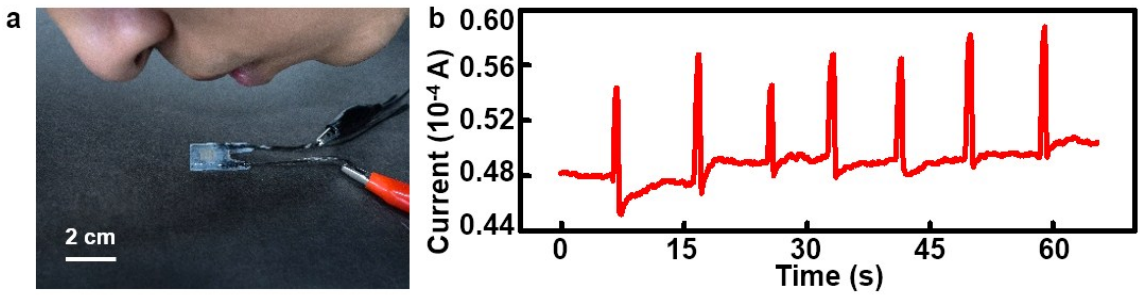


**Figure S7.** The breathing sensing performance of sensors. (a) Photograph demonstrating the LDW-carbonized sensor detecting breathing force. (b) Current response plot of the device resulting from breathing.

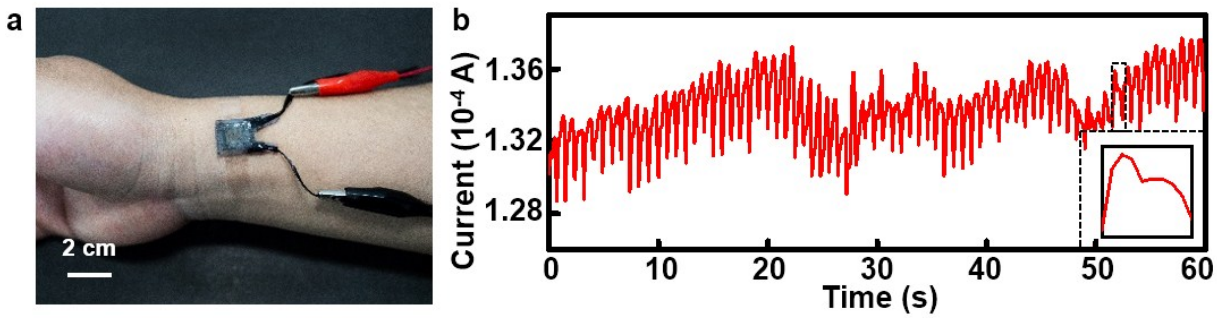


**Figure S8.** The pulsing sensing performance of sensors. (a) Photograph demonstrating the LDW-carbonized sensor attached to a student's wrist for measuring the radial artery pressure waveforms. (b) Current–time plot of the radial artery pressure waveforms.

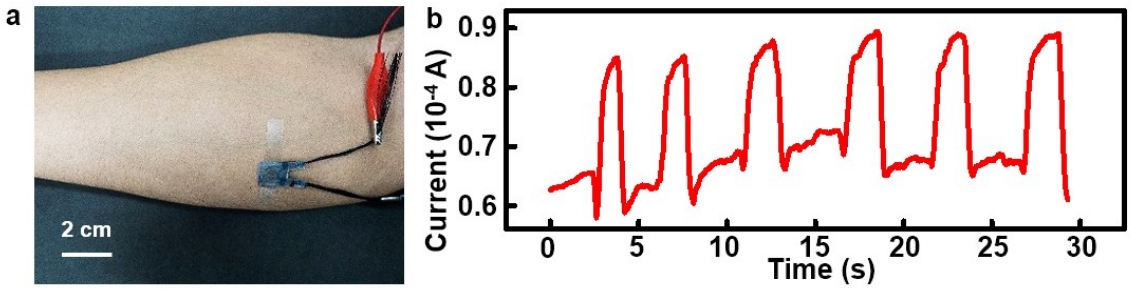


**Figure S9.** The muscle movement sensing performance of sensors. (a) Photograph demonstrating the LDW-carbonized sensor attached to the inner side of the forearm for measuring the muscle motion signal. (b) Current–time plot of the measured signals generated from the contraction and relaxation of muscles.

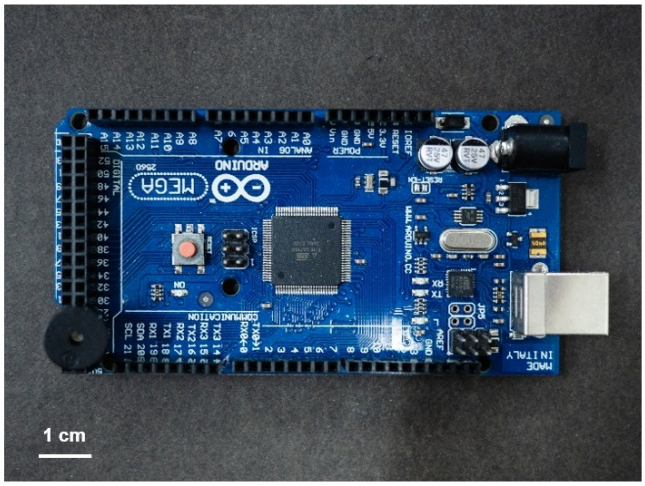


**Figure S10.** Photograph demonstrating the arduino electronic platform for collecting the sensor signals.

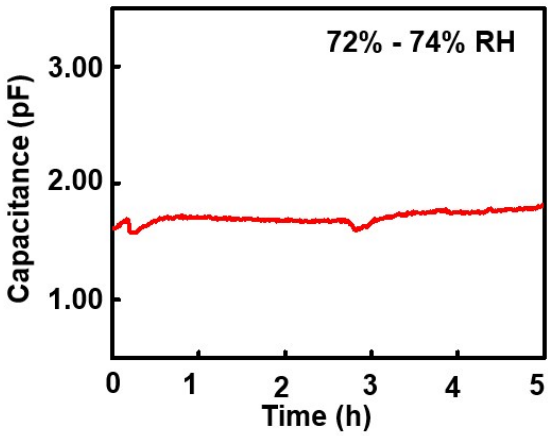


**Figure S11.** The stability of the humidity sensing of the LDW-fabricated humidity sensor in a range of 72%-74%RH for 5 hours.

**Table S1.** The ratio of the elements in the carbonized cardboard.

| Element | Wt % | At % |
|---|---|---|
| C K | 46.77 | 55.89 |
| N K | 01.43 | 01.46 |
| O K | 43.39 | 38.93 |
| Na K | 00.70 | 00.44 |
| Mg K | 00.29 | 00.63 |
| Al K | 01.18 | 00.17 |
| Si K | 01.47 | 00.63 |
| Cl K | 00.38 | 00.15 |
| K K | 00.59 | 00.22 |
| Ca K | 03.80 | 01.36 |